Acta Cryst. (1981). A37, 414–421

Electrostatic Molecular Interaction from X-ray Diffraction Data. I. Development of the Method; Test on Pyrazine

BY GRANT MOSS* AND DIRK FEIL

Chemical Physics Laboratory, Twente University of Technology, PO Box 217, 7500 *AR Enschede, The Netherlands*

(*Received* 1 *July* 1980; *accepted* 17 *December* 1980)

Abstract

Electrostatic interaction is often an important part of the total interaction between molecules. It depends on the electron density distribution in the participating molecules, which can, in principle, be determined by X-ray diffraction methods. A method is described to calculate the electrostatic interaction between two nonpenetrating molecules by adding the pair-wise interaction between the constituent atoms. The molecular electron density distribution is expressed in terms of the densities corresponding with spherical atoms and deformations according to Hirshfeld's method. The electrostatic interaction between the various deformation densities is replaced by the interaction between the atomic multipole moments corresponding with the deformation densities. Application of the method to pyrazine, $C_4H_4N_2$, showed qualitative agreement with results based on quantum-chemical calculations.

1. Introduction

At an increasing rate, papers are published on the accurate determination of the electron density distribution in crystals, by means of X-ray diffraction. At the present state of the art, the effects of chemical bonding can be recognized and occasionally an attempt is made to compare the observed quantities with the results of quantum-chemical calculations. It is generally assumed that the electron density distribution in van der Waals crystals of rigid molecules is a superposition of the distributions of the isolated molecules. Thus the electron density distribution in these molecules can, in principle, be derived from diffraction data.

The various moments of the charge distribution in a molecule, some of which can be determined experimentally by various methods, depend in a unique way on the electron density distribution. Consequently, they provide a test for the results obtained by diffraction methods. Coppens, Guru Row, Leung, Stevens, Becker & Yang (1979) have shown that dipole moments, determined from diffraction data, correspond well with the moments derived from dielectric measurements. Since very few data on higher moments exist, no comparison has been made as yet.

Kihara (1963) has shown the importance of multipole moments in molecular interaction. From the work of Mulder & Huiszoon (1977) on the interaction between azabenzene molecules, it follows that the electrostatic interaction between two molecules, whose centers are 15 atomic units apart, is of the same order of magnitude as the dispersion interaction. Buckingham (1959) showed how the electrostatic interaction between nonoverlapping molecules can be expressed in terms of the moments of the charge distributions of these molecules. Thus, knowledge of the charge distribution, or of its moments, is an essential requirement for the calculation of molecular interaction.

The dispersion interaction is usually handled by the method of atom–atom potentials. In this method the interaction energy is considered to be the sum of the interaction energies between the constituent atoms. Since electrostatic properties of a molecular charge distribution can be described in terms of atomic charges and (atomic) multipole moments, the electrostatic interaction can equally well be separated in atomic contributions. When experimental interaction data are used to derive atom–atom potentials, the resulting potentials contain both dispersion and electrostatic contributions. Consequently, the potentials are only transferable to molecules with a similar charge distribution. A more satisfying procedure is to calculate the dispersion energy with atom–atom potentials based on dispersion energy calculations and to add the electrostatic energy explicitly.

This has recently been applied by Hirshfeld & Mirsky (1979), who calculated the electrostatic energy of a number of small molecules. They compare several models to account for the charge distribution in the molecule. Mulder & Huiszoon (1977) have shown, however, that anisotropic contributions tend to cancel in the lattice sum. So it may be expected that the results

* Present address: Medical Foundation of Buffalo, Inc., 73 High Street, Buffalo, New York 14203, USA.

0567-7394/81/030414-08$01.00

of Hirshfeld & Mirsky are not representative for dimer interactions.

The present study is directed towards calculating the electrostatic interaction between two identical molecules, from data obtained by X-ray diffraction on crystals of these molecules.

Hirshfeld (1971) developed a method to describe the electron density distribution in a crystal in terms of density distributions centered on the atomic sites. Superimposed on the density of unperturbed spherical atoms is the deformation density. When two molecules are separated by a distance of a few van der Waals radii, the contributions to the electrostatic interaction by the spherical atoms vanish and only the deformation density remains important. The present method is based on Hirshfeld's method of charge analysis. The method is tested on pyrazine. For this compound an extensive single-crystal diffraction data set is available (de With, Harkema & Feil, 1976). The results of the calculation of the electrostatic energy from experimental data can be compared with the results obtained by Mulder & Huiszoon (1977) who based their calculations on double-ζ-quality wave functions.

2. Method

Following Hirshfeld (1971), we can write the molecular electron density distribution as

$$\rho(\mathbf{r}) = \sum_i \left[\rho_s^{(i)}(\mathbf{r}_i) + \sum_{n,k} \rho_{n,k}^{(i)}(\mathbf{r}_i) \right], \tag{1}$$

in which $\mathbf{r}_i = \mathbf{r} - \mathbf{R}_i$, $\mathbf{R}_i$ being the position vector of atom i; $\rho_s^{(i)}$ is the density distribution of some model of the neutral atom i; and $\rho_{n,k}^{(i)}$ represents a deformation of the atomic electron density with respect to this model density distribution. The summation extends over all atoms in the molecule.

The atomic deformation functions $\rho_{n,k}$ are of the general form

$$\rho_{n,k}^{(i)}(\mathbf{r}_i) = c_{n,k}^{(i)} N_n r_i^n e^{-\alpha_i r_i} \cos^n \theta_{n,k}. \tag{2}$$

$\theta_{n,k}$ is the angle between the vector $\mathbf{r}_i$ and a specified polar axis (n,k), n is an integer between 0 and 4, and α is a parameter that governs the radial breadth of the deformation functions on each type of atom. N_n is a normalizing factor.

The functions of second order or higher are hybrid functions. Thus the six functions with $n = 2$ are linear combinations of a monopole function ($n = 0$) and five independent functions with the same radial dependence and an angular dependence $Y_{lm}(\theta,\varphi)$ with $l = 2$ and $m = 0, \pm 1, \pm 2$. In the same way the functions with $n = 4$ contain terms with $n = 2$ and $n = 0$. Thus, three terms, with radial dependence $e^{-\alpha r}$, $r^2 e^{-\alpha r}$ and $r^4 e^{-\alpha r}$ respectively, are present to describe spherical deformations of the charge distribution of the various atoms.

Hirshfeld developed a program to obtain the deformation parameters $c_{n,k}^{(i)}$ and α_i and the structure parameters $\mathbf{R}_i$ from diffraction intensities by means of a least-squares procedure.

The electrostatic energy between atom A and atom B is given by

$$E = e^2 \int \left\{ \left[-\rho_A(\mathbf{r}_1) + \sum_{i \in A} Z_i \, \delta(\mathbf{r}_1 - \mathbf{R}_i) \right] \times \left[-\rho_B(\mathbf{r}_2) + \sum_{j \in B} Z_j \, \delta(\mathbf{r}_2 - \mathbf{R}_j) \right] \times (4\pi\varepsilon_0 |\mathbf{r}_1 - \mathbf{r}_2|)^{-1} \right\} \mathrm{d}^3\,\mathbf{r}_1 \, \mathrm{d}^3\,\mathbf{r}_2, \tag{3}$$

in which $Z_i|e|$ is the nuclear charge of atom i, $\delta(\mathbf{r})$ is the Dirac delta function and ε_0 is the permittivity of vacuum. The potential at a point outside the atomic region due to the spherical electron density distribution, $\rho_s^{(i)}$, is equal in magnitude and opposite in sign to the potential due to the nucleus i. Consequently, in the expression for the electrostatic interaction between two nonpenetrating molecules only the deformation densities occur

$$E = \sum_{i \in A} \sum_{j \in B} \sum_{n,k} \sum_{m,l} e^2 \times \int \{ [\rho_{n,k}^{(i)}(\mathbf{r}_1 - \mathbf{R}_i) \, \rho_{m,l}^{(j)}(\mathbf{r}_2 - \mathbf{R}_j)] \times (4\pi\varepsilon_0 |\mathbf{r}_1 - \mathbf{r}_2|)^{-1} \} \, \mathrm{d}^3\,\mathbf{r}_1 \, \mathrm{d}^3\,\mathbf{r}_2. \tag{4}$$

Following Buckingham (1959), the calculation of electrostatic interaction between two charge distributions can be considerably simplified by replacing the charge distributions by point multipoles. The definition of the various multipole moments is given in Appendix *A*. Appendix *B* shows how these multipole moments can be derived from the deformation functions as given in (2). It should be noted, however, that here the multipole moments represent the deformation charges of the various atoms and not the molecular charge density. Fig. 1 shows that beyond the van der Waals radius the potential due to a deformation density distribution $\sum_{n,k} \rho_{n,k}^{(i)}$ does not significantly deviate from the potential due to a limited set of multipoles on nucleus i. It should be noted that the calculation is based on interaction between pseudoatoms, *i.e.* units whose charge distribution deviates only slightly from spherical symmetry. Hirshfeld's program allows the determination of deformation functions up to fourth order ($n = 4$).

Finally, Appendix *C* gives the contributions to the interaction energy by the different pairs of multipole moments.

3. The deformation model: choice of parameters

The potentially large number of deformation functions necessary to describe the electron density distribution

in pyrazine can be reduced by the following symmetry considerations.

(1) The point-group symmetry of the pyrazine molecule imposed by the space-group symmetry *Pmnn* is $2/m$.

(2) In addition, the molecule is found to be planar, resulting in *mmm* (D_{2h}) symmetry (de With *et al.*, 1976).

Often the type and quality of the experimental data on which the refinement is based does not warrant the determination of subtle deformations of the atoms. This means that the corresponding parameters cannot be fixed with sufficient accuracy and are better dropped. Since considerable correlation exists between various parameters, reduction of the parameter set introduces bias in the results.

Owing to the diffuse character of its density distribution, the hydrogen atom hardly contributes to the scattering by the various deformation functions. Therefore, functions beyond first order for the hydrogen atom are not included. For the same reason only an isotropic temperature factor was used to describe the thermal motion of the hydrogen atom. The scattering factors of Stewart, Davidson & Simpson (1965) were used to represent the spherical density ρ_s^H.

For the carbon and nitrogen atoms deformation functions up to fourth order are included. Since the parameters describing the thermal motion of the atoms are strongly correlated with the even-order deformation functions, the zero-order function was omitted in one of the models. The number of parameters can be further reduced by introducing constraints. Since the coefficients of the first-order deformation functions of hydrogen are strongly coupled to the positional parameters of this atom, the use of a full set of deformation functions does not improve the description of the electron density distribution. Quantum chemistry indicates that on bond formation the rotational symmetry of the hydrogen atom about the bond axis is approximately preserved. Consequently this symmetry has been used in the refinement. The appearance of the electron density difference map (Fig. 2) suggests that the N–C and C–C bonding regions are very similar. By assuming the density about the C atom to have *mm* symmetry, we have taken this into account. The validity of the assumption is confirmed by the residual map, in which both bonding regions mentioned above have the same, flat, appearance. The atomic scattering factors listed in *International Tables for X-ray Crystallography* (1974) were used for the neutral undisturbed atoms. The information on the unit cell is given in Table 1; Table 2 summarizes the parameters of the models used.

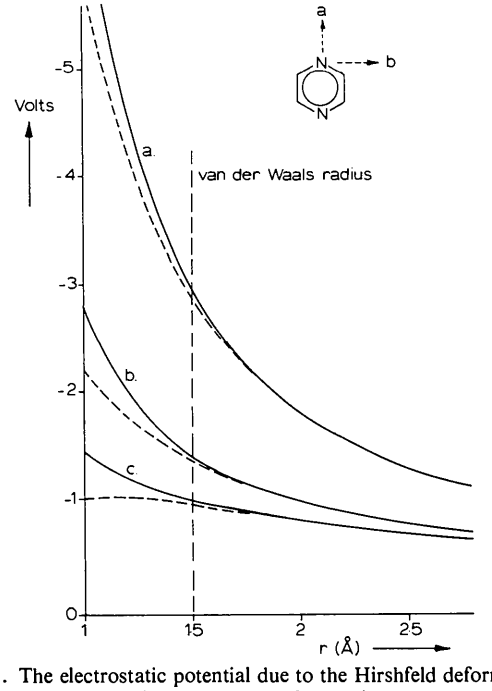

Fig. 1. The electrostatic potential due to the Hirshfeld deformation function on the nitrogen atoms of pyrazine. The potential is calculated in three perpendicular directions, two of which are indicated in the figure. The third direction, **c**, is perpendicular to the plane of the molecule. The solid line gives the exact potential, *i.e.* the potential based on deformation densities up to fourth order, extended in space, whereas the dashed line gives the potential due to point multipoles up to fourth order on the site of the nitrogen atom.

Table 1. *Unit-cell information at* 184 K

Here and in the following tables, standard deviations are given in parentheses.

$a =$ 9·325 (4) Å	Space group no. 58, *Pmnn*
$b =$ 5·850 (2)	$Z = 2$
$c =$ 3·733 (1)	Point symmetry of the
$V =$ 203·6 (2) Å^3	atoms: C, H:1; N:2

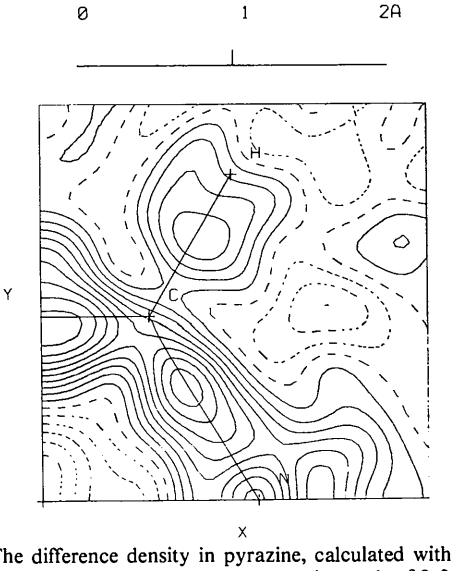

Fig. 2. The difference density in pyrazine, calculated with $F_{obs} - F_{spherical\,atom}$ as input. The contours are at intervals of 0·05 e Å^{-3}. The contours are solid and dashed for positive and negative densities respectively.

Table 2. *Parameters of the refinement models*

The anisotropic temperature factors used are:

$\exp[-2\pi^2(h^2a^{*2}U_{11} + k^2b^{*2}U_{22} + l^2c^{*2}U_{33} + 2hka^*b^*U_{12} + 2hla^*c^*U_{13} + 2klb^*c^*U_{23})]$.

The isotropic temperature factor, used for H, is given by $\exp(-8\pi^2\bar{U}\sin^2\theta/\lambda^2)$.

Structure parameters	Common to all models			
Positional parameters				
N	x/a			
C	$x/a, y/b, z/c$			
H	$x/a, y/b, z/c$			
Thermal parameters				
N	$U_{11}, U_{22}, U_{33}, U_{23}$			
C	$U_{11}, U_{12}, U_{13}, U_{22}, U_{23}, U_{33}$			
H	U			
Scale factor	k			
Deformation density parameters	Models			
	01X	11X	11X 4·0	11X 5·25
Radial exponent α	$\alpha_N, \alpha_C, \alpha_H$	$\alpha_N, \alpha_C, \alpha_H$	α_N, α_C	α_N, α_C
Fixed exponent α_H	–	–	4·0 Å^{-1}	5·25 Å^{-1}
Zero-order function on	C, N, H	H	H	H
First-order function on	C, N, H	C, N, H	C, N, H	C, N, H
Second-, third- and fourth-order functions on	C, N	C, N	C, N	C, N

4. Results of the electron density analysis

The structural and deformation parameters were determined by minimizing $\sum_H W(\mathbf{H})[F^2_{obs}(\mathbf{H}) - F^2_{model}(\mathbf{H})]^2$ in which $W(\mathbf{H})$ and $F^2_{obs}(\mathbf{H})$ are the weight factors and squared structure factors, respectively, determined and used by de With *et al.* (1976).

In Table 3 the results of refinements using various deformation models are listed together with the results of a high-order (HO) refinement (model 8 by de With *et al.*).

The refined C–H bond lengths are much longer than the accepted value of 1·08 Å (Kay, Okaya & Cox, 1971; de With *et al.*, 1976).

The positional parameters of the carbon atom differ slightly from the HO refinement. The nitrogen parameters and scale factor are in good agreement for all refinements. The C–H bond length is strongly correlated with the radial exponent α_H. So by choosing an appropriate value of α_H, we can obtain the correct C–H distance with virtually no increase in disagreement between model and observation. A series of refinements were carried out with fixed α_H parameters, ranging from 4·0 to 6·0. The best C–H bond length was obtained with $\alpha_H = 5{\cdot}25$ for model 11X (C–H = 1·078 Å) and with $\alpha_H = 5{\cdot}00$ for model 01X (C–H = 1·114 Å). Table 4 shows the various atomic and molecular multipole moments, together with the disagreement factor R_w, defined as

$$R_w \equiv \frac{\sum_H W(\mathbf{H})|F^2_{obs}(\mathbf{H}) - F^2_{model}(\mathbf{H})|^2}{\sum_H W(\mathbf{H})F^2_{obs}(\mathbf{H})}.$$

The final R_w factors are rather high, reflecting the relatively low quality of the data, which in turn is due to the poor mechanical properties of pyrazine crystals. The internal consistency of the intensities I, expressed by the factor $R_I \equiv \sum(I - \bar{I})/\sum I$, in which the summation extends over all measured reflexions and in which $\bar{I}$ is the corresponding weighted average, was reported to be 2·5%. Table 4 shows that there is no preference for a particular model to represent the experimental data.

Hirshfeld's analysis is based on the model of a molecule as consisting of independent deformed atoms, each with its own temperature factor. The resulting

Table 3. *Comparison of high order (HO[1]) and deformation density refinements of the experimental data of de With et al.* (1976)

Positional parameters are $\times 10^5$ for C, N, $\times 10^3$ for H, thermal $\times 10^4$ for C, N, $\times 10^3$ for H. The anisotropic temperature factors used are

$\exp[-2\pi^2(h^2a^{*2}U_{11} + k^2b^{*2}U_{22} + l^2c^{*2}U_{33} + 2hka^*b^*U_{12} + 2hla^*c^*U_{13} + 2klb^*c^*U_{23})]$.

		HO[1]	Model 11X	Model 01X
H	x	128 (1)	140 (2)	139 (2)
	y	305 (6)	338 (6)	338 (16)
	z	194 (3)	232 (4)	232 (4)
	U	43 (2)	49 (15)	42 (16)
C	x	7440 (7)	7459 (6)	7457 (6)
	y	17774 (10)	17812 (13)	17808 (13)
	z	12193 (24)	12185 (13)	12182 (13)
	U_{11}	292 (3)	290 (2)	291 (2)
	U_{22}	285 (3)	285 (2)	285 (2)
	U_{33}	381 (4)	390 (2)	389 (3)
	U_{12}	−30 (2)	−34 (2)	−34 (2)
	U_{23}	19 (2)	13 (2)	14 (2)
	U_{13}	−28 (2)	−31 (1)	−32 (1)
N	x	14987 (8)	14992 (12)	14990 (11)
	U_{11}	225 (3)	224 (2)	223 (2)
	U_{22}	335 (3)	340 (3)	337 (3)
	U_{33}	452 (5)	454 (4)	452 (4)
	U_{23}	61 (3)	54 (3)	54 (3)
Scale		40·97 (46)	41·2 (2)	40·9 (4)
WRF (%)		6·0	4·70	4·69
GoF		1·68	1·76	1·76
α_H (Å^{-1})		–	6·3 (5)	5·9 (5)
α_C		–	6·4 (4)	6·2 (4)
α_N		–	7·1 (1·0)	6·7 (9)
C–H 10l (Å)		0·94 (1)	1·190	1·186
θ^{mol}_{xx} (a.u.)			−5·66	−5·30
θ^{mol}_{yy}			9·09	8·86
$\theta^{mol}_{zz} \equiv -(\theta_{xx} + \theta_{yy})$			(−3·43)	(−3·56)

deformation parameters, together with vanishing temperature factors, can be used to synthesize a deformation density that presumably represents a molecule at rest. The result for model 11X is found in Fig. 3. Excluding the region within approximately 0·3 Å of the atomic site, the standard deviation of the deformation density calculated from the least-squares covariance matrix is in general below 0·05 e Å^{-3}. The residual density, calculated with the difference between observed structure factors and structure factors based on model 11X with $\alpha_H = 5{\cdot}25$, is shown in Fig. 4.

Table 4. *Variation of* C–H *bond length and atomic and molecular moments with the exponent on hydrogen for model* 11X *refinements*

Atomic multipoles are in units of (+e), (+e Å) and (+e Å^2). Molecular moments are in atomic units. The definition of axes for the moments is the same as that given in Table 2.

		α_H (Å^{-1})					
Parameter		4·0	4·5	5·0	5·25	5·5	6·0
C–H (Å)		0·967	0·988	1·030	1·076	1·134	1·203
H	q	−0·180	−0·158	−0·098	−0·014	0·098	0·215
	μ_x	0·049	0·056	0·068	0·074	0·074	0·059
	μ_y	0·082	0·094	0·115	0·125	0·125	0·099
C	q	0·211	0·248	0·200	0·115	−0·003	−0·152
	μ_x	0·066	0·064	0·053	0·030	−0·008	−0·063
	μ_y	0·109	0·104	0·087	0·049	−0·013	−0·102
	θ_{xx}	−0·042	−0·040	−0·037	−0·032	−0·026	−0·025
	θ_{xy}	−0·013	−0·016	−0·025	−0·050	−0·091	−0·145
	θ_{yy}	−0·055	−0·056	−0·063	−0·083	−0·119	−0·174
	θ_{zz}	0·097	0·097	0·101	0·115	0·145	0·199
N	q	−0·182	−0·195	−0·202	−0·201	−0·188	−0·126
	μ_x	−0·042	−0·041	−0·040	−0·044	−0·048	−0·052
	θ_{xx}	−0·095	−0·093	−0·089	−0·086	−0·081	−0·078
	θ_{yy}	−0·091	−0·089	−0·088	−0·092	−0·100	−0·123
	θ_{zz}	0·186	0·182	0·177	0·178	0·181	0·200
Scale		40·91 (25)	40·88 (24)	40·87 (24)	40·98 (24)	41·10 (25)	41·27 (20)
θ_{xx}^{mol}		−5·05	−5·38	−5·79	−6·17	−6·39	−5·79
θ_{yy}^{mol}		2·84	4·24	6·35	8·35	10·26	9·97
θ_{zz}^{mol}		2·21	1·14	−0·56	−2·18	−3·87	−4·18
WRF (%)		4·73	4·73	4·73	4·73	4·72	4·70

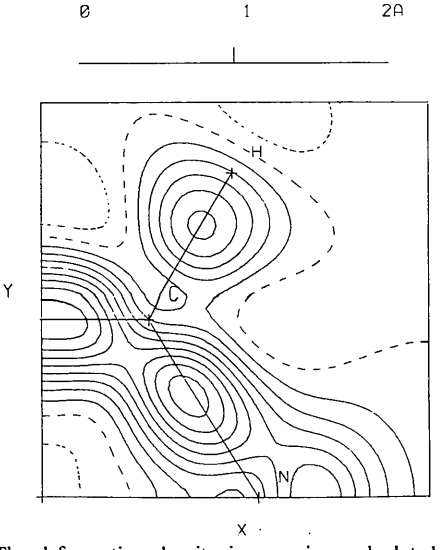

Fig. 3. The deformation density in pyrazine, calculated with the deformation parameters of model 11X (see Table 2). Contours as in Fig. 2.

Almlöf, Roos, Wahlgren & Johansen (1973) carried out a quantum-chemical calculation of pyrazine using a single determinant wavefunction with double-ζ-quality molecular orbitals. The basis set consisted of the following contracted Gaussians: C, N (7·3/4·2) and H (4·1/2·1). By putting two molecules in a unit cell, the same structure factors were calculated as in the experimental set. The difference density, based on the difference between these molecular structure factors and the structure factors calculated with spherical standard atoms, is shown in Fig. 5.

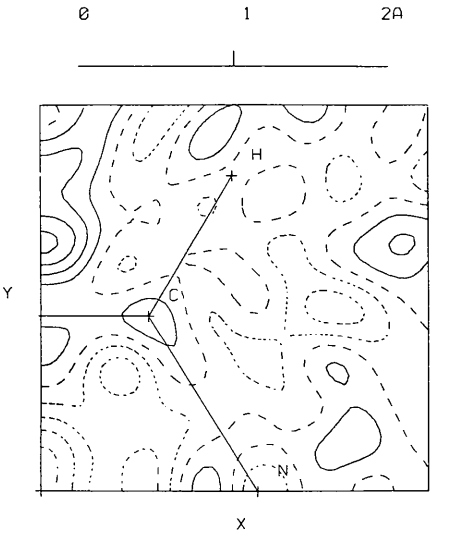

Fig. 4. The residual density of pyrazine, indicating the difference in electron density as observed and the density according to model 11X. Contours as in Fig. 2.

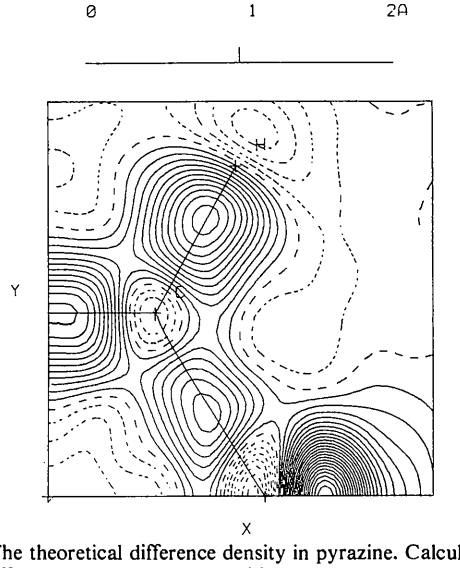

Fig. 5. The theoretical difference density in pyrazine. Calculated is the difference between the densities based on the molecular wavefunction and on spherical atoms. Contours as in Fig. 2. No thermal smearing has been applied.

The correspondence with the deformation density of Fig. 3 is quite good. Noticeable differences can be found in C–C, C–N and nitrogen lone-pair regions. Similar discrepancies have been observed by de With *et al.* (1976) in calculations using a Hartree–Fock–Slater wave function. Bats & Feil (1977) have noticed a similar discrepancy between theoretical and experimentally determined lone-pair density. They attributed the deviation to the use of incorrect atomic parameters as derived from a high-order refinement. In the present case, in which the deformation density is explicitly accounted for in the model, this explanation does not apply. Other features in the experimental density distribution do not appear to be significantly different from the usual results.

5. The calculation of the electrostatic interaction

From the expressions given in Appendix *C*, the electrostatic energy was calculated for two pyrazine molecules in different orientations with respect to each other and with a distance of 15 a.u. (0·793 nm) between the centers of mass. In Fig. 6 the results are shown for the various refinements. The theoretical result of Mulder & Huiszoon (1977) is also shown for comparison.

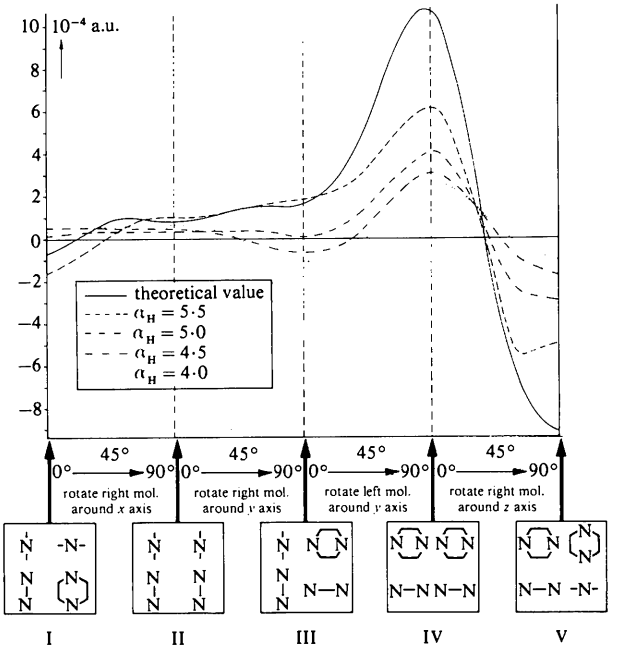

Fig. 6. The electrostatic interaction energy between two pyrazine molecules whose centers are 15 a.u. apart. The relative orientation of the molecules is indicated at the bottom of the figure. The various dashed curves are for the electron density description according to model 11X with different values of the exponent of the hydrogen deformation function. The solid curve indicates the theoretical value obtained by Mulder & Huiszoon (1977).

We notice a qualitative agreement between the interaction energies based on experimental data and on the wave function. At the same time we see that models, whose quality could not be distinguished on the basis of experimental data, show quite different results with respect to the interaction energy. Moreover, these results do differ considerably from the theoretical values as obtained by Mulder & Huiszoon (1977). The latter fact does not surprise us, since the electron density distributions, particularly in the nitrogen lone-pair region, differed as well.

6. Discussion of the results and conclusions

The qualitative agreement between the theoretical and experimental results indicate that the method proposed offers promise for obtaining essential data for the calculation of electrostatic interaction. In view of the fact that no other experimental method suggests itself for obtaining the higher multipole moments required for the calculation of the orientation-dependent interaction, the result is comforting. At the same time the discrepancies are of such a magnitude that further research is necessary to find its origin. The first question that arises is the choice between models that fit the experimental data equally well. Although it can be assumed that the range of choice will reduce with increasing quality of experimental data, additional criteria to base the choice on are quite welcome. The second question deals with the adequacy of Hirshfeld's method to describe the molecular electron density distribution. If the structure factors are without error and the density distribution corresponds with a molecule at rest, with no temperature factors to absorb any inadequacy of the model, the parameters of an extended model should be determinable with great accuracy. If, in addition, the structure factors are based on a particular wave function of the molecule the resulting interaction energies should closely correspond with interaction energies calculated with perturbation theory, the procedure used by Mulder & Huiszoon (1977).

In a following paper the results of the analysis of a set of theoretical structure factors will be reported.

APPENDIX *A*
Definition of multipole moments

For a discrete distribution of point charges e_j, at positions $\mathbf{r}_j$ (r_{jx}, r_{jy}, r_{jz}) with respect to some origin, the various multipole moments are defined by

$$q = \sum_j e_j$$

$$\mu_\alpha = \sum_j e_j r_{j\alpha}$$

$$\theta_{\alpha\beta} = \tfrac{1}{2}\sum_j e_j[3r_{j\alpha}\, r_{j\beta} - r^2\,\delta_{\alpha\beta}]$$

$$\Omega_{\alpha\beta\nu} = \tfrac{1}{2}\sum_j e_j[5r_{j\alpha}\, r_{j\beta}\, r_{j\nu} - r_j^2(r_{j\alpha}\,\delta_{\beta\nu} + r_{j\beta}\,\delta_{\alpha\nu} + r_{j\nu}\,\delta_{\alpha\beta})]$$

$$H_{\alpha\beta\nu\eta} = \tfrac{1}{8}\sum_j e_j[35r_{j\alpha}\, r_{j\beta}\, r_{j\nu}\, r_{j\eta} - 5r_j^2(r_{j\beta}\, r_{j\nu}\,\delta_{\alpha\eta} + r_{j\alpha}\, r_{j\nu}\,\delta_{\beta\eta} + r_{j\alpha}\, r_{j\beta}\,\delta_{\nu\eta} + r_{j\alpha}\, r_{j\eta}\,\delta_{\beta\nu} + r_{j\beta}\, r_{j\eta}\,\delta_{\alpha\nu} + r_{j\nu}\, r_{j\eta}\,\delta_{\alpha\beta}) + r_j^4(\delta_{\alpha\eta}\,\delta_{\nu\beta} + \delta_{\alpha\nu}\,\delta_{\eta\beta} + \delta_{\alpha\beta}\,\delta_{\nu\eta})],$$

where α, β and γ denote any choice of x, y and z and δ is the Kronecker symbol. The corresponding results for a continuous charge distribution are obtained by replacing the summation by an integration over the charge distribution.

APPENDIX *B*
Multipole moments from the Hirshfeld deformation model

The k's deformation density component of order n is given by

$$\rho_{n,k}(\mathbf{r}) = C_{n,k}\frac{\alpha^{n+3}(n+1)}{4\pi(n+2)!}\, r^n\, e^{-\alpha r}\cos^n\theta_{n,k}, \quad (B1)$$

where the direction specified by the indices (n,k) is defined in terms of a local set of Cartesian axes **(X,Y,Z)**. We define a second Cartesian frame $(\mathbf{K}_x,\mathbf{K}_y,\mathbf{K}_z)$, where $\mathbf{K}_z$ is parallel to the direction (n,k), and $\mathbf{K}_x$ is defined through the relation $\mathbf{K}_x = \mathbf{K}_z \times \mathbf{Z}$ (see Fig. 7).

In the $(\mathbf{K}_x,\mathbf{K}_y,\mathbf{K}_z)$ frame the axial symmetry of $\rho_{n,k}$ about $\mathbf{K}_z$ implies that there will be only one independent component in each multipole moment tensor (Buckingham, 1959). Denoting the contribution from $\rho_{n,k}$ to the independent component of a general multipole of order m by $O^{m,n}_{\mathbf{K}_z}$, we can write

$$O^{m,n}_{\mathbf{K}_z} = \int_{\text{vol}} r^m\, P_m(\cos\theta_{n,k})\rho_{n,k}\,\mathrm{d}^3\,\mathbf{r}. \quad (B2)$$

Inserting $(B1)$ in this expression, we have to calculate

$$O^{m,n}_{\mathbf{K}_z} = C_{n,k}\frac{\alpha^{n+3}(n+1)}{2(n+2)!}\int_0^\infty \mathrm{d}r\, r^{m+n+2}\, e^{-\alpha r} \times \int_0^\pi P_m(\cos\theta)\cos^n\theta\,\mathrm{d}\cos\theta. \quad (B3)$$

The right-hand integral $\int_{-1}^{1} P_m(x)x^n\,\mathrm{d}x$ can be found by expressing x^n as a series of Legendre polynomials. Nonvanishing results are obtained when m and n are both even or both odd. As an example we give the even case:

$$x^n = \frac{1}{n+1}P_0(x) + \sum_{k=1}^{n}(4k+1) \times \frac{\left(\frac{n}{2}+k\right)!}{\left(\frac{n}{2}-k\right)!}\frac{2^{2k}(n)!}{(n+2k+1)!}P_{2k}(x).$$

Equation $(B3)$ becomes

$$O^{m,n}_{\mathbf{K}_z} = C_{n,k}\frac{\alpha^{n+3}(n+1)}{2(n+2)!}\frac{(m+n+2)!}{\alpha^{m+n+3}} \times 2^{m+1}n!\frac{\left(\frac{n+m}{2}\right)!}{\left(\frac{n-m}{2}\right)!} = C_{n,k}\frac{m+n+2}{n+2}\frac{2^m\left(\frac{n+m}{2}\right)!}{\alpha^m\left(\frac{n-m}{2}\right)!}\sigma_{n,m},$$

where $\sigma_{n,m} = \begin{cases} 1 \text{ for } n \geq m \text{ and} \\ \quad n,m \text{ both even or both odd} \\ 0 \text{ otherwise.} \end{cases}$

The tensor $O^{m,n}_{\mathbf{K}_z}$, of rank m and calculated in the $(\mathbf{K}_x,\mathbf{K}_y,\mathbf{K}_z)$ frame, has now to be transformed to the local frame **(X,Y,Z)**, which is common to all deformation density components centered on one atom. This transformation can be carried out by two consecutive rotations as shown in Fig. 7.

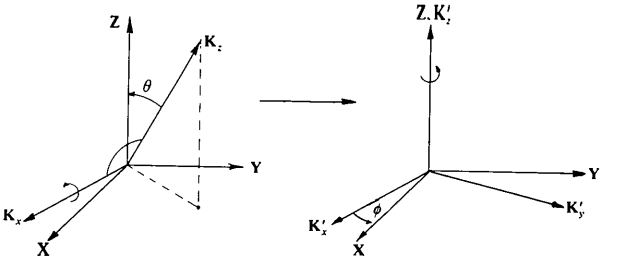

Fig. 7. The transformation from the deformation frame $(\mathbf{K}_x,\mathbf{K}_y,\mathbf{K}_z)$ to a local atomic frame **(X,Y,Z)**.

APPENDIX C
Expressions for the interaction energy between the various multipoles

$$U_{m-m} = \frac{q^{(1)} q^{(2)}}{4\pi\varepsilon_o R}$$

$$U_{m-d} = \frac{R_\alpha}{4\pi\varepsilon_o R^3}\left[q^{(2)}\mu_\alpha^{(1)} - q^{(1)}\mu_\alpha^{(2)}\right]$$

$$U_{m-q} = \frac{R_\alpha R_\beta}{4\pi\varepsilon_o R^5}\left[q^{(2)}\theta_{\alpha\beta}^{(1)} + q^{(1)}\theta_{\alpha\beta}^{(2)}\right]$$

$$U_{m-o} = \frac{R_\alpha R_\beta R_\gamma}{4\pi\varepsilon_0 R^7}\left[q^{(2)}\Omega_{\alpha\beta\gamma}^{(1)} - q^{(1)}\Omega_{\alpha\beta\gamma}^{(2)}\right]$$

$$U_{m-h} = \frac{R_\alpha R_\beta R_\gamma R_\eta}{4\pi\varepsilon_0 R^9}\left[q^{(2)}H_{\alpha\beta\gamma\eta}^{(1)} + q^{(1)}H_{\alpha\beta\gamma\eta}^{(2)}\right]$$

$$U_{d-d} = \frac{1}{4\pi\varepsilon_0 R^3}\left[\mu_\alpha^{(1)}\mu_\alpha^{(2)} - \frac{3}{R^2}\left(\mu_\alpha^{(1)}R_\alpha\right)\left(\mu_\beta^{(2)}R_\beta\right)\right]$$

$$U_{d-q} = \frac{5R_\alpha R_\beta R_\eta}{4\pi\varepsilon_0 R^7}\left[\mu_\eta^{(1)}\theta_{\alpha\beta}^{(2)} - \mu_\eta^{(2)}\theta_{\alpha\beta}^{(1)}\right] + \frac{2R_\alpha}{4\pi\varepsilon_0 R^5}\left[\theta_{\alpha\beta}^{(1)}\mu_\beta^{(2)} - \theta_{\alpha\beta}^{(2)}\mu_\beta^{(1)}\right]$$

$$U_{d-o} = -\frac{7R_\alpha R_\beta R_\gamma R_\eta}{4\pi\varepsilon_0 R^9}\left[\mu_\eta^{(2)}\Omega_{\alpha\beta\gamma}^{(1)} + \mu_\eta^{(1)}\Omega_{\alpha\beta\gamma}^{(2)}\right] + \frac{3R_\alpha R_\beta}{4\pi\varepsilon_0 R^7}\left[\mu_\gamma^{(2)}\Omega_{\alpha\beta\gamma}^{(1)} + \mu_\gamma^{(1)}\Omega_{\alpha\beta\gamma}^{(2)}\right]$$

$$U_{q-q} = \frac{35\theta_{\alpha\beta}^{(1)}\theta_{\gamma\eta}^{(2)}}{12\pi\varepsilon_o R^9}R_\alpha R_\beta R_\gamma R_\eta - \frac{5\theta_{\alpha\beta}^{(2)}\theta_{\alpha\gamma}^{(1)}}{3\pi\varepsilon_0 R^7}R_\beta R_\gamma + \frac{\theta_{\alpha\beta}^{(1)}\theta_{\alpha\beta}^{(2)}}{6\pi\varepsilon_0 R^5},$$

where summation over repeated subscripts is implied.

References

ALMLÖF, I., ROOS, B., WAHLGREN, U. & JOHANSEN, H. (1973). *J. Electron. Spectrosc. Relat. Phenom.* **2**, 51–74.

BATS, J. W. & FEIL, D. (1977). *Chem. Phys.* **22**, 175–181.

BUCKINGHAM, A. D. (1959). *Q. Rev. Chem. Soc.* **13**, 183–214.

COPPENS, P., GURU ROW, T. N., LEUNG, P., STEVENS, E. D., BECKER, P. & YANG, Y. W. (1979). *Acta Cryst.* A**35**, 63–72.

HIRSHFELD, F. L. (1971). *Acta Cryst.* B**27**, 769–781.

HIRSHFELD, F. L. & MIRSKY, K. (1979). *Acta Cryst.* A**35**, 366–370.

International Tables for X-ray Crystallography (1974). Vol. IV. Birmingham: Kynoch Press.

KAY, M. I., OKAYA, Y. & COX, D. E. (1971). *Acta Cryst.* B**27**, 26–33.

KIHARA, T. (1963). *Adv. Chem. Phys.* **4**, 147–188.

MULDER, F. & HUISZOON, C. (1977). *Mol. Phys.* **34**, 1215–1235.

STEWART, R. F., DAVIDSON, E. R. & SIMPSON, W. T. (1965). *J. Chem. Phys.* **42**, 3175–3187.

WITH, G. DE, HARKEMA, S. & FEIL, D. (1976). *Acta Cryst.* B**32**, 3178–3184.

Acta Cryst. (1981). A**37**, 421–425

Exact Method for the Calculation of Pseudorotation Parameters P, τ_m and Their Errors. A Comparison of the Altona–Sundaralingam and Cremer–Pople Treatment of Puckering of Five-Membered Rings

BY S. T. RAO, E. WESTHOF AND M. SUNDARALINGAM

Department of Biochemistry, College of Agricultural and Life Sciences, University of Wisconsin–Madison, Madison, Wisconsin 53706, *USA*

(*Received* 4 *February* 1980; *accepted* 19 *December* 1980)

Abstract

A comparison of the two methods available for describing the puckering of five-membered rings – the Altona–Sundaralingam (A–S) [Altona & Sundaralingam (1972). *J. Am. Chem. Soc.* **94**, 8205–8212] pseudorotation parameters τ_m, P and the Cremer–Pople (C–P) [Cremer & Pople (1975). *J. Am. Chem. Soc.* **97**, 1354–1358] puckering parameters q, φ – shows that they are the same for all practical purposes but both have minor shortcomings. In the A–S method, the value of τ_m is somewhat dependent on the choice of

0567-7394/81/030421-05$01.00